Applied Catalysis B: Environmental 306 (2022) 121130

Contents lists available at ScienceDirect

Applied Catalysis B: Environmental

journal homepage: www.elsevier.com/locate/apcatb

Enhanced photocatalytic removal of ozone by a new chlorine-radical-mediated strategy

Lei Wang [a,b,1], Jian Guan [a,1], Hao Han [b], Mingyue Yao [b], Jian Kang [b], Meng Peng [a], Desheng Wang [b], Jiayu Xu [a,*], Jiming Hao [a]

[a] Tsinghua University, School of Environment, Beijing 100084, China
[b] Research Institute of Chemical Defense, State Key Laboratory of NBC Protection for Civilian, Beijing 102205, China

ARTICLE INFO

Keywords:
TiO_2
Photocatalysis
O_3
Chlorine radical

ABSTRACT

In this study, the photocatalytic chlorine-radical-mediated reaction dramatically enhanced the catalytic activity of TiO_2 for ozone removal, which was different from traditional photocatalytic mechanism driven by hydroxyl radicals. Chlorinated TiO_2 was prepared using the sol-gel method and modified through surface chlorination. The ozone-removal efficiency was up to 99.9% over the chlorinated TiO_2 under UV light, which was 2.5 times that of bare TiO_2. Moreover, experiments also showed that chlorinated TiO_2 possessed excellent water-resistance and reusability. Characterization results unveiled that the chlorine is attached to the surface of TiO_2 in the form of Ti–Cl bonds, which can capture holes to form·Cl. Subsequently, it was proven that the chain transfer reaction initiated by·Cl was mainly responsible for the remarkable improvement in the photocatalytic conversion of ozone. This new photocatalytic mechanism driven by chlorine radical opens up a new field of ozone removal by photocatalysis.

1. Introduction

Although ozone plays a critical role in protecting the life on the Earth from the ultraviolet (UV) radiation of the sun, the ozone present near the ground is a hazardous pollutant. Because of its strong oxidation capacity, ozone can damage cell membranes and nuclei and cause diseases [1,2]. Ozone near the ground is generated by photochemical reactions involving NO_x and VOCs emitted from vehicles or factories. Besides, the leakage or production of ozone from special industrial equipment, such as disinfection apparatus or photocopiers in indoor environment, may lead to a high concentration of ozone that can severely endanger human health [3]. Studies have shown that even a low ozone concentration of 0.1 ppm can cause discomforts such as skin irritation, coughing, and lacrimation [4]. Therefore, ozone elimination has always been one of the research focuses in the field of environment and catalysis.

Photocatalysis is considered as one of the most promising strategy for contaminant removal because of mild reaction condition, high effectiveness, non-consumption of chemical reagents, and low energy consumption [5,6]. Titanium dioxide (TiO_2), as the most common material, has been widely exploited because of its good chemical and photonic stability and relatively good reactivity [7–9]. In TiO_2 photocatalysis, O_3 and surface hydroxyl groups react through photogenerated carriers to generate free radicals and active groups such as O_3^-, O_4^-, and·OH. Finally O_3 is converted to O_2 through free-radical chain reaction [10–12]. The reaction mechanism is depicted in formulas 1–5.

$$TiO_2 \rightarrow h^+ + e^- \quad (1)$$

$$O_3 + e^- \rightarrow O_3^- \quad (2)$$

$$OH^- + h^+ \rightarrow OH \quad (3)$$

$$O_3 + OH \rightarrow O_4^- + H^+ \quad (4)$$

$$O_3 + O_3^- \rightarrow O_4^- + O_2 \quad (5)$$

However, since the conversion of ozone on bare TiO_2 is low [13], improving the photocatalytic activity is the main research direction in this field. Thus far, research on ozone conversion by TiO_2 photocatalysis was mostly based on metal loading. Noble metals such as Au, Pt, and Pd [14–16] promote charge transfer and reduce the surface potential, thereby enhancing the photocatalytic effect. Transition metals such as

* Corresponding author.
E-mail address: jiayu_tsinghua@163.com (J. Xu).
[1] These authors have contributed to this work equally.

https://doi.org/10.1016/j.apcatb.2022.121130
Received 29 November 2021; Received in revised form 14 January 2022; Accepted 20 January 2022
Available online 22 January 2022

Fe and Cu repeatedly combined with photoelectrons and holes to switch their valence states, so as to promote charge transfer [17,18]. However, compared with other catalysts, TiO_2-based photocatalysts are still less efficient, which is attributed to the complex path based on the interaction between O_3 and OH radical. [15,19]. Therefore, there is no further enhancement of ozone conversion via the traditional photocatalysis driven by OH radical.

In fact, the problem of ozone elimination near the ground is similar to an environmental issue that requires an urgent solution—ozone hole in the atmosphere caused by ozone depletion. Over the last few decades, a large number of chlorofluorocarbons used as refrigerants leaked into the atmosphere, generating chlorine free radicals under the excitation of UV light. These radicals then interacted with ozone to generate oxygen. Free-radical chain reaction is extremely efficient; the chlorine itself does not change, and hence, the original dynamic balance in natural conversion between ozone and oxygen is broken, causing a large loss of ozone and forming a void. TiO_2 photocatalysis is also a type of free-radical reaction, and can produce free radicals to participate in the reaction by light irradiation. In addition, the reaction rate of chlorine radical with ozone is much faster than that of hydroxyl [20,21]. Therefore, introduction of chlorine free radicals in the photocatalysis process is equivalent to introducing an efficient atmospheric reaction on the catalyst surface, and these radicals will greatly facilitate the ozone conversion. Yuan et al. studied the application of surface-chlorinated $BiOBr/TiO_2$ for photocatalysis, believing that chlorine radicals have lower energy than hydroxyl radicals but are more active and can be used to activate $–CH_3$ [22] or C–H [23]. The combination of TiO_2 and chlorine radicals has not yet been reported for ozone conversion.

This is the first study in which the atmospheric process of ozone depletion through chlorine radicals was introduced into photocatalytic ozone conversion. Under UV irradiation, new active groups on chlorinated TiO_2 photocatalyst generate chlorine radicals. These photo-induced chlorine radicals, instead of hydroxyl radicals, drive a more efficient chain reaction to convert ozone.

2. Materials and methods

2.1. Materials

Isopropyl titanate was from America Sigma-Aldrich Inc. The agents for surface treatment, hydrochloric, sulfuric and nitric acid, were supplied by Sinopharm Chemical Reagent Co., Ltd (China). All chemicals are analytic grade and used as purchased without further purification.

2.2. Catalyst preparation

TiO_2 was prepared by an improved sol–gel method [24]. At room temperature, 15.0 mL isopropyl titanate was slowly added dropwise to 180 mL of 0.1 mol/L sulfuric acid solution under violent stirring, and stirring was continued for 24 h. After dialysis, pH was adjusted to 3–4 to obtain a uniform transparent sol. After the sol was dried, it was ground in an agate mortar to obtain dry gel powder, which was calcined at 450 °C for 3 h to obtain nano-TiO_2, which is denoted as T. The calcination temperature was adjusted to 250 °C, 350 °C, 550 °C, and 650 °C, and the products were denoted as T250, T350, T550, and T650, respectively.

Chlorinated TiO_2 was prepared by an impregnation method: 1 g TiO_2 powder was immersed in 1 mL concentrated hydrochloric acid and sealed and kept in the dark for 24 h. Subsequently, it was exposed to allow it to volatilize for 12 h and then dried at 50 °C after washing with water. The obtained chlorinated T is denoted as TC.

In addition, TiO_2 impregnated with concentrated sulfuric acid and concentrated nitric acid, i.e., TS and TN, respectively, were prepared by the same method for comparison with TC.

2.3. Photocatalytic experiments

Ozone was the target pollutant in the experiments. The aim was to study the photocatalytic capacity of the prepared catalytic material in gas-phase reactions. As shown in Fig. 1, ozone was generated using a self-made UV excitation device. Air flowed through a 185-nm UV lamp to excite ozone and a humidifier to adjust humidity. After adjusting the device to achieve a flow rate of 100 mL/min and an initial ozone concentration of 100 ppm, the ozone gas was inserted into a quartz reaction tube with a dimeter of 0.4 cm. The tube contained 0.2 g of catalyst (the length of catalyst is about 1.8 cm) and then the irradiated surface area is about 1.13 cm^2. The light source was a xenon lamp with continuous wavelength of 300–800 nm (AULTT CEL-HXUV300). The light intensity near the reactor was about 650 mW/cm^2 (measured by CEL-NP2000-2A). The gas pipeline was connected, and the UV lamp was turned on after balanced adsorption. After the reaction started, the experimental setup was maintained at room temperature, and the ozone concentration in the exhaust gas was recorded every 30 min (2B Model 106 M). In addition, except for the humidity experiment, other experiments were under feed gas condition with an average relative humidity (RH) of 18%.

2.4. Characterization

The X-ray diffraction (XRD), with a scanned 2θ range from 10° to 80°, was measured on Rigaku UItima IV diffractometer using Cu radiation. ZEISS Gemini 300 scanning electron microscope (SEM) was utilized to test the morphology of samples. Transmission Electron Microscope (TEM) and Energy-dispersive X-ray spectroscopy (EDS) was performed by FEI TalosF200x. The photocurrent and Mott–Schottky test were performed at an Epsilon electrochemical workstation. Shimadzu UV-3600 spectrophotometer was used to test UV-Vis DRS with $BaSO_4$ as a reference. Content of chlorine was tested on Thermo Fisher ICS5000 ion chromatography. Photoluminescence spectra (PL) was performed on Edinburgh FSK1000 spectrometer. X-ray photoelectron spectroscopy (XPS) was tested on Bruker Alpha. Fourier transform–infrared spectroscopy (FT-IR) was performed by Nicolet NEXUS 670. Electron paramagnetic resonance (EPR) was test by Bruker A300 with N-tert-Butyl-α-phenylnitrone (PBN) of capture agent.

3. Result and discussion

3.1. Morphological characterization

The XRD patterns of the synthesized TiO_2 samples are shown in Fig. 2. The diffraction peaks of T250, T350, T and TC samples corresponded perfectly with the anatase phase (JSPDS card No. 21-1272) without obvious indication of impurities [25], and the diffraction peak

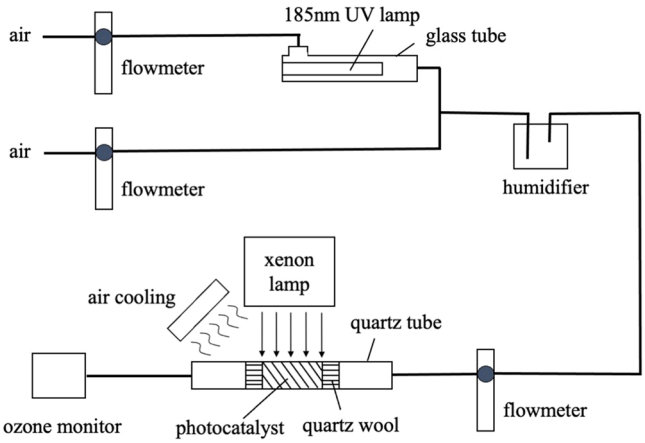

Fig. 1. The scheme of ozone generation and photocatalytic reactor.

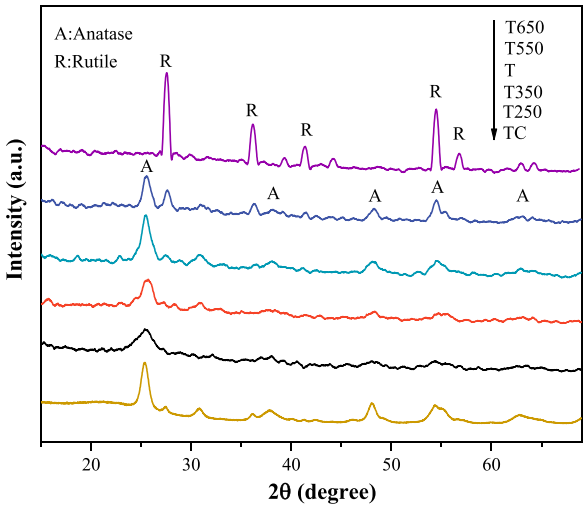

Fig. 2. XRD patterns of the synthesized samples.

intensity of anatase phase increased gradually with the increase of temperature. The diffraction peak intensity of phase increases gradually with the increase of temperature, which indicated that T samples had high crystallinity and may have better photocatalysis performance [26]. T550 samples were mixture of anatase phase and rutile phase. T650 samples were corresponded perfectly with rutile phase (JSPDS card No. 21-1276), which indicated that with the increase of treatment temperature, anatase gradually transitioned to rutile. Comparing the T and TC, it could be found that chlorination had no obvious effect on the crystal form of the catalyst.

The morphology of T and TC samples were examined by the SEM and TEM. As shown in Fig. S1, T and TC photocatalysts were both of block structure. TEM results in Figs. 3a and 3b exhibited that there was no significant change in particle size and mean particle sizes of T and TC samples were 13.4 nm and 13.6 nm, respectively. The interplanar spacing of T and TC were both 0.346 nm, corresponding to the anatase (101) plane, which was in good accordance with the results of the XRD patterns. The results of electron microscopy showed that chlorination had no obvious effect on the morphology of the photocatalysts.

The elemental EDX mapping of sample clearly demonstrated the existence of Ti, O and Cl on TC surface (Fig. 3c–f), and the distribution of these elements was quite uniform. All data fully proved that the chlorinated TiO_2 photocatalyst was successfully prepared.

3.2. Photocatalysis performance

The photocatalytic properties of TC, TN, TS, and TiO_2 for removing ozone were tested and compared in Fig. 4a. TiO_2 exhibited photocatalytic capacity, and the ozone-conversion rate could reach 40%. There was no obvious deactivation in the 4-h reaction period. However, neither TiO_2 dark reaction nor simple UV irradiation could effectively decompose ozone. Under identical conditions, the ozone-conversion rate of TC is extremely high and exceeds 99.9% owing to surface modification of the catalyst, which does not work without irradiation. To explore the role of acidification, experiments were performed with TN and TS. Results showed that photocatalytic conversion rate of TN against ozone was almost the same as that of TiO_2, which was about 40%. The catalytic

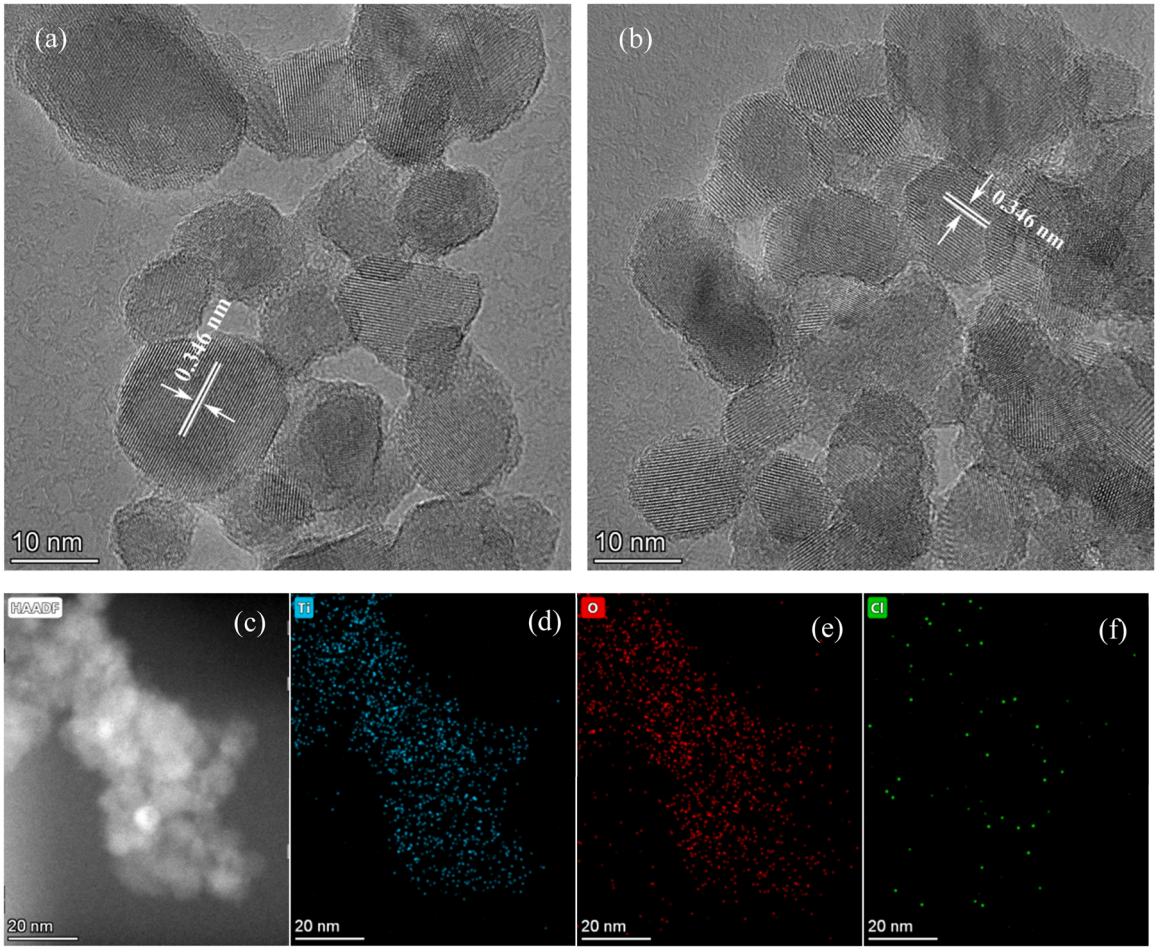

Fig. 3. TEM images of (a) T sample (b) TC sample, (c) HAADF image and (d) Ti, (e) O, (f) Cl EDS elemental mapping of TC sample.

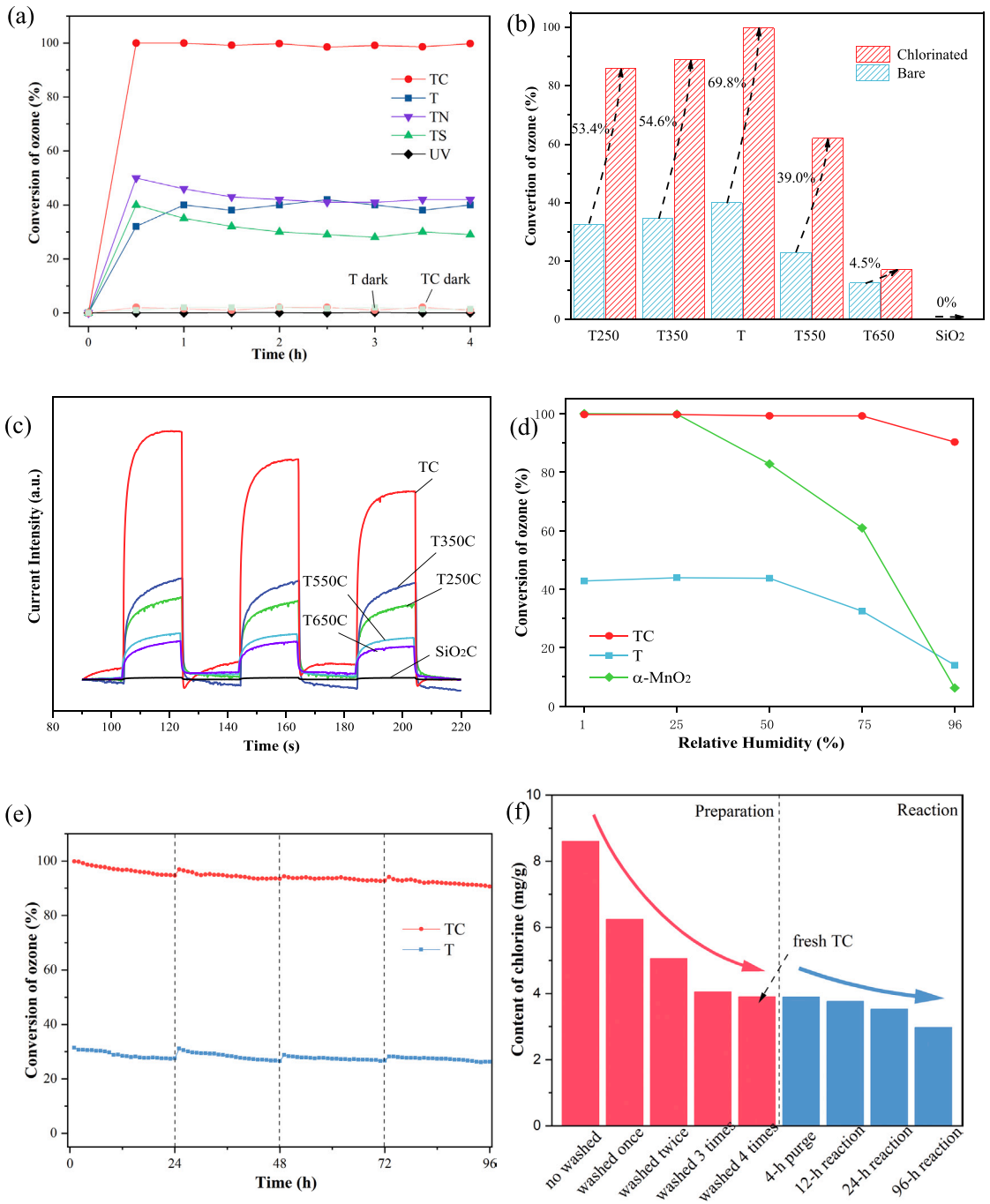

Fig. 4. (a) Conversion of ozone on TC, TS, TN, and TiO_2; (b) Conversion of ozone on TiO_2 with different calcination temperatures; (c) Photocurrent of chlorinated SiO_2 and TiO_2 with different calcination temperatures; (d) Conversion of ozone on TiO_2 at different humidity; (e) 4*24-h photocatalytic activity of T and TC samples at RH75%; (f) Content of chlorine on TC after washing and reaction.

performance of TS was worse than that of TiO_2, with a 4-h conversion rate of 28%. This showed that acidification of the TiO_2 photocatalyst played a small role on ozone decomposition, and the Cl is the main factor contributing to the significant increase in activity.

To explore the coupling effect of Cl and photocatalysis, the effect of TiO_2 calcined at different temperatures with surface chlorination was examined. As shown in Fig. 4b, as the calcination temperature increased, the ozone-conversion performance of bare TiO_2 tended to first increase and then decrease. TiO_2 calcined at 450 °C showed the highest activity, with a conversion rate of about 40%, while TiO_2 calcined at 650 °C only had a conversion rate less than 10%. Surface chlorination promoted the photocatalytic effect of various TiO_2 materials, and their efficiencies were positively correlated with the ozone-conversion rate of bare TiO_2. Meanwhile, the results of photocurrent in Fig. 4c and performance test results were in agreement. TC sample had the maximum photocurrent and most carriers. It is obvious that under the same chlorination conditions, the stronger the original photocatalytic capability in photocatalysts, the greater the improved effect of surface chlorination, which is 53.4%, 54.6%, 69.8%, 39.0% and 4.5% respectively. This indicated that the quantum efficiency of the carrier directly determined the reaction performance of the surface chlorine group. This finding further proved that the reaction between the surface chlorine group and ozone was fully embedded in the photocatalytic process. In addition, owing to the lack of photocatalytic properties, chlorination cannot promote the

reactivity of SiO_2 against ozone, which corresponded with the above speculation. Hence, unlike previous metal-supported modification methods [19], chlorine groups must combine with photocatalytic process to function and cannot be excited directly by UV light.

Water-resisting property test was necessary in the field of catalytic degradation of ozone. As exhibited in Fig. 4d, TC photocatalyst showed excellent water-resisting property, while α-MnO_2, as the most common catalyst for ozone decomposition [27], showed undesirable water-resisting property. When the humidity was less than 96%, the conversion rates of TC photocatalyst all exceeded 99%. The conversion rates of α-MnO_2 and T photocatalyst seriously decreased when the humidity was more than 50% RH. Under high humidity conditions (96% RH), a 4-h conversion rate of TC photocatalyst was 90.3%, while T photocatalyst and α-MnO_2 just could decompose 14.1% and 6.3% of ozone, respectively. Therefore, TC photocatalyst could effectively decompose ozone in all humidity ranges.

Reusability and stability were significant characteristics of practical application and 4 * 24-h reaction experiments under 75% RH condition were conducted. At the end of each cycle, the catalyst was taken out, evenly shaken and refilled, in order to reduce the adverse effects of single-side light on the photocatalytic materials. As shown in Fig. 4e, in the first cycle, the conversion of ozone dropped from 99% to 97%, which dropped from 98% to 94% in the second cycle, from 95% to 92% in the third cycle, and from 93% to 89% in the last cycle. Overall, after 96 h reaction, the loss of TC performance is about 11%. Under the same condition, the conversion on pure TiO_2 dropped from 32% to 27%.

Subsequently, the chlorine content of TC in preparation and reaction have been tested and the results are shown in Fig. 4f. Being washed once, the chlorine dropped from 8.6 mg/g to 6.24 mg/g and tended to be constant after multiple washing, about 3.9–4.0 mg/g. It is mainly because there is a large amount of chlorine after immersing and water washing can remove the unstable chlorine in the form of HCl. The more stable Cl-Ti will not affected by washing and purging in the dark. In the process of photo-reaction, the chlorine content dropped from 4.0 mg/g to 3.76 mg/g after 12-h light irradiation, 3.52 mg/g after 24-h, and eventually 2.97 mg/g after 96-h reaction. It can be inferred that chlorine radicals generated by light will be slowly lost with the airflow, which is the main reason for the degradation of the performance.

Moreover, the XRD and XPS of photocatalyst after reaction were applied to research the structural and surface changed before and after reaction, which were shown by Fig. S2. The XRD peaks were in the same place after reaction, which demonstrated that the crystal structure of TC sample was not destroyed. The XPS results showed that Cl was still attached to the surface after the reaction and there is appropriate loss of chlorine. This may be because the chlorine after reaction with ozone returns to the surface [22]. The above results proved its excellent stability and reusability.

3.3. Optical and electrochemical properties

The UV–vis DRS results showed the optical absorption properties of T and TC samples in Fig. 5a. The optical absorption capacity of the T and TC samples was almost the same when the wavelength is less than 400 nm. Moreover, by the Kubelka–Munk equation [28], the gap energies of T and TC could be calculated as 2.95 eV respectively. The PL spectra and photocurrent result of both T and TC samples were shown in Fig. S3 and there is little difference in PL spectra and photocurrent result between the two results.

The flat band potentials of both T and TC samples were computed by Mott–Schottky plot. As shown in Fig. 5b, T and TC samples were both identified as n-type semiconductors due to their positive slope and the flat band potentials were −0.80 V vs. Ag/AgCl and −0.90 V vs. Ag/AgCl respectively, which is −0.20 V and −0.30 V vs. RHE. For n-type semiconductors, the flat band potential was 0.1 V greater than conduction band (CB). Hence, the CB potentials of T and TC samples were −0.30 V and −0.40 V vs. RHE respectively. According to the UV–vis DRS, the band gap energies of T and TC samples were both 2.95 eV. Correspondingly, the valence band (VB) potentials of samples could be calculated to be 2.65 V and 2.55 V vs. RHE by formula: $E_{VB} = E_{CB} + Eg$, respectively [29]. The VB potential of TC (+2.55 eV) was more positive than redox potential of Cl/Cl^- (+2.47 eV) [30,31], so photogenerated holes could oxidize Cl to·Cl. The evidence above proved that hydrochloric acid treatment had no significant effect on the optical and electrochemical properties of TiO_2, which indicated that acidification has little effect and Cl is the main factor contributing to the significant increase in activity, consistent with the experimental results.

3.4. Surface analysis

To clarify the connection mode of Cl on the TiO_2 photocatalyst surface, infrared absorption spectrum and XPS were performed. Fig. 6 showed the infrared absorption spectrum of T and TC. The two absorption peaks near 3630 and 3690 cm^{-1} were attributed to the O–H stretching vibration [32], which proved that there were hydroxyl groups on the catalyst surface. For TC sample, a broad and strong peak appeared between 2800 and 3600 cm^{-1}, reflecting the characteristic absorption of bound water and a lot of hydrogen bonds [33]. The absorption peak near 530 cm^{-1} was attributed to Ti–Cl stretching vibration [34]. A comparison of the infrared spectra of the two materials showed that chlorination changed the catalyst surface properties with the weakened hydroxyl peak, enhanced bound water absorption peak and new Ti–Cl peak, indicating that TC had better water absorption ability, less hydroxyl and

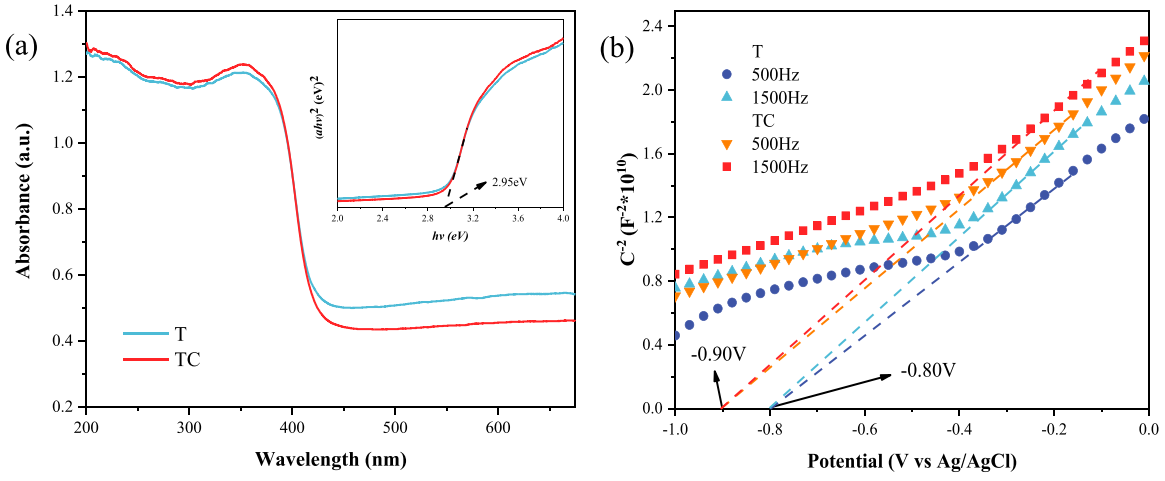

Fig. 5. (a) UV–Vis DRS and bandgap energies; (b) Mott–Schottky plots of T and TC.

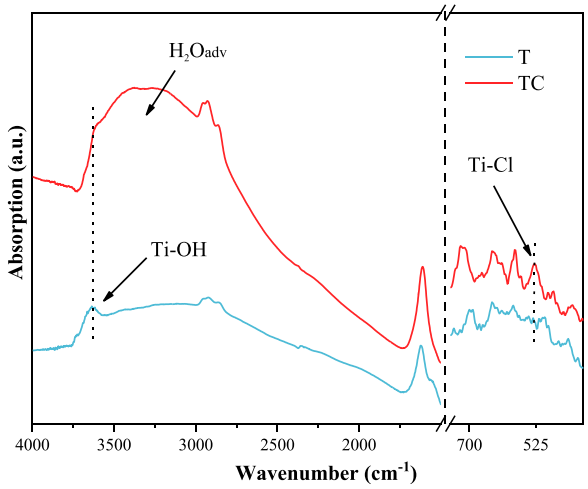

Fig. 6. FT–IR patterns of T and TC samples.

emerging Ti–Cl bonds. Enhanced water absorption ability was most likely because of the excessive increase in the number of acidic sites. In addition, according to literature and infrared absorption spectrum, it was speculated that Cl replaced the surface hydroxyl group of TiO_2 [22].

Fig. 7a exhibited the O 1s XPS peak of TC in detail. After peak fitting, double peaks were obtained, corresponding to lattice oxygen (530.1 eV) and surface-adsorbed water and hydroxyl (532.2 eV) [35]. The narrow XPS spectrum of Cl element was shown in Fig. 7b and the Cl 2p peak showed two components at 198.0 eV and 199.7 eV, which were assigned to Cl $2p_{3/2}$ and Cl $2p_{1/2}$, respectively [36]. The peak at 198.0 eV was generally considered as the evidence for the presence Ti–Cl bonds, which meant Cl ion was absorbed on TiO_2 surface [37,38]. Based on these XPS and infrared spectroscopy results, it could be inferred that Cl partially replaced the binding site of HO–Ti to generate Cl–Ti, and the reaction is as follows: $HCl + HO - Ti \rightarrow Cl\text{–}Ti + H_2O$.

3.5. Reaction mechanism

The reaction between chlorine and ozone in nature was the main cause for the creation of the ozone hole in the atmosphere. Studies has shown [39] that under the irradiation of UV light at high altitude, the chlorine in chloroflurocarbons (CFCs) will be excited to generate chlorine radicals, which convert ozone to oxygen (One chlorine radical can destroy about 100,000 ozone molecules). In the paper, this atmospheric reaction has been introduced into photocatalysis on the surface of TiO_2. Chlorine radicals, instead of traditional OH radicals, generated in the photocatalytic process will drive the chain transfer reaction to decompose ozone efficiently. EPR technology was employed, and PBN was used as a capture agent to study the new free radicals generated by TC in the UV reaction process. The results were shown in Fig. 8. Under UV irradiation, obvious octet peaks were detected, and even the fine structure of each group of peaks is observable. This is the characteristic signal generated by the PBN capture of chlorine radicals, which confirms the previous speculation [40].

Combining the existing semiconductor light excitation theory and the reaction mechanism of creation of the ozone hole, the photocatalytic reaction mechanism of TC against ozone can be deduced, as shown in Scheme 1. Under UV light irradiation, TiO_2 VB electrons are transferred to the CB, forming photogenerated electrons and photogenerated holes (Formula 7). A part of electrons and holes undergo recombination annihilation, while the remaining is transferred to the catalyst surface to drive the photocatalytic free-radical reaction. The Cl on the TiO_2 surface combines with holes and loses an electron to generate·Cl (Formula 8) [23,41].·Cl interacts with O_3 to generate an·OCl and an O_2 molecule (Formula 9).·OCl reacts with O_3 again to generate two O_2 molecules. Simultaneously,·OCl is reconverted to·Cl (Formula 10), thus completing the cycle of free-radical chain transfer reaction [39,42]. In this work, the mechanism was introduced to decompose ozone for the first time. For its implementation, chlorine is embedded into the TiO_2 solid surface and then the h^+ generated by TiO_2 light excitation is converted into·Cl [23].

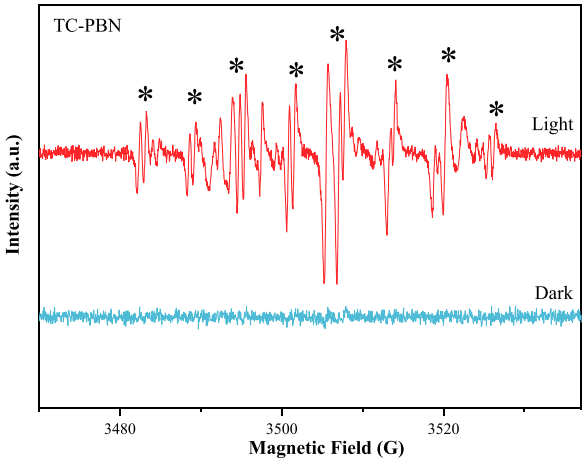

Fig. 8. EPR pattern of TC-PBN (Cl) under UV light irradiation.

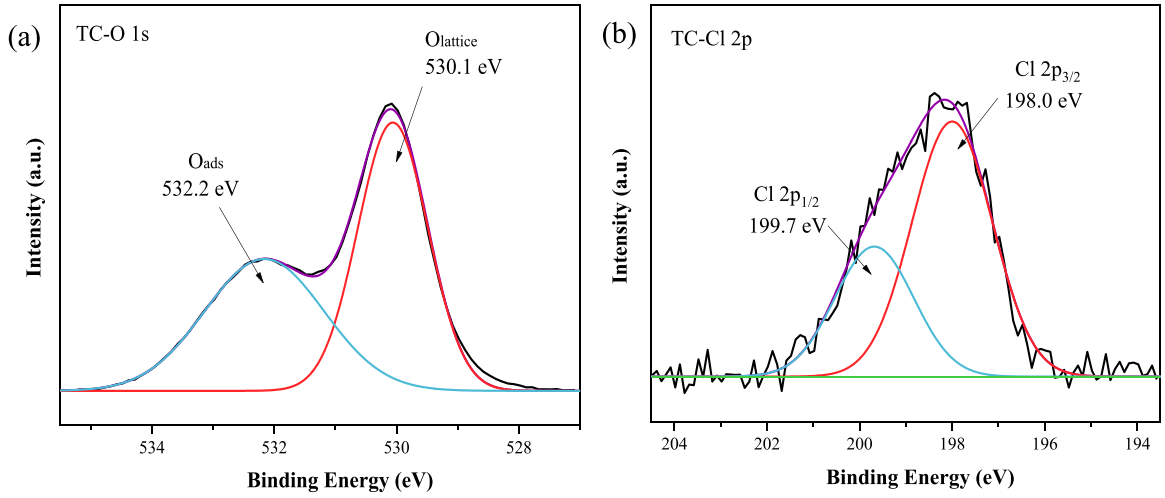

Fig. 7. XPS spectra of (a) O element and (b) Cl element.

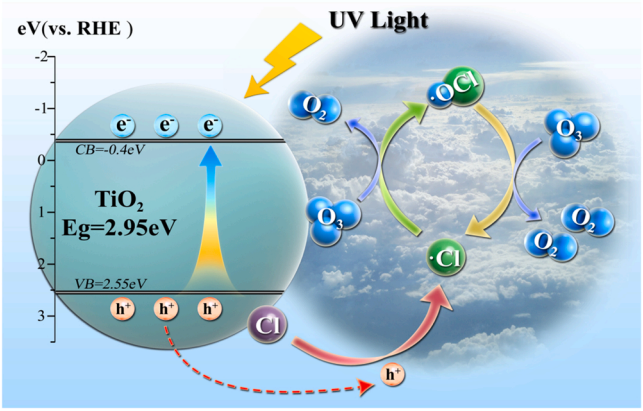

Scheme 1. Photocatalytic mechanism of ozone conversion over TC.

Thus, the O_3 conversion reaction is driven. TC catalyzes O_3 by introducing new free radicals in heterogeneous reactions, thereby replacing the mechanism of $\cdot O_2^-$ and ·OH in the traditional photocatalysis. There is no precedent of adoption of such a mechanism in the study of TiO_2 modification.

$$TiO_2 \rightarrow h^+ + e^- \quad (7)$$

$$Cl + h^+ \rightarrow \cdot Cl \quad (8)$$

$$\cdot Cl + O_3 \rightarrow \cdot OCl + O_2 \quad (9)$$

$$\cdot OCl + O_3 \rightarrow \cdot Cl + 2O_2 \quad (10)$$

4. Conclusion

The TC catalytic material prepared and surface modified in this work has extremely high O_3 photocatalytic reaction activity. Under UV irradiation, 100 ppm ozone can be completely eliminated, which is 2.5 times that of bare TiO_2. With improvement in the efficiency of the TiO_2 photon, surface chlorination has increasingly significant promotion effect, which indicates surface chlorination is a reaction mechanism highly coupled with the photocatalytic process. Meanwhile, the photocatalyst have excellent water-resisting property and reusability. Characterization results have shown that TiO_2 is excited by light to produce h^+, which captures the electrons of Ti–Cl to convert Cl into·Cl and in turn drives the free-radical reaction in a manner similar to the process of ozone hole formation in the atmosphere. In this reaction,·Cl has extremely high activity against O_3, and hence it replaces the traditional photocatalytic $\cdot O_2^-$ and·OH to become the main active species in the O_3 reaction. Thus, TiO_2 exhibits a high conversion capacity. This work has obtained a high-efficient photocatalyst for ozone decomposition and provided the new photocatalytic system with surface chlorination, which will yield innovative ideas for the enhancement of ozone photocatalysis performance.

CRediT authorship contribution statement

Lei Wang: Conceptualization, Methodology, Investigation, Resources, Writing – original draft, Visualization. **Jian Guan:** Methodology, Validation, Investigation, Writing – original draft, Visualization. **Hao Han:** Investigation. **Mingyue Yao:** Investigation. **Jian Kang:** Writing – review & editing. **Meng Peng:** Resources. **Desheng Wang:** Writing – review & editing. **Jiayu Xu:** Resources, Supervision, Project administration, Funding acquisition. **Jiming Hao:** Resources, Supervision, Project administration, Funding acquisition.

Declaration of Competing Interest

The authors declare that they have no known competing financial interests or personal relationships that could have appeared to influence the work reported in this paper.

Acknowledgements

This work was supported by the National Key Scientific and Technological Project (DQGG0302-04). Thanks Prof. Shi Hu, Prof. Xiuqiang Xie, Prof. Yanhui Zhang, and Prof. Xiaoqing Liu for their help in revising. For xyz.

Appendix A. Supporting information

Supplementary data associated with this article can be found in the online version at doi:10.1016/j.apcatb.2022.121130.

References

[1] X. Lu, J. Hong, L. Zhang, O.R. Cooper, M.G. Schultz, X. Xu, T. Wang, M. Gao, Y. Zhao, Y. Zhang, Severe surface ozone pollution in China: a global perspective, Environ. Sci. Technol. Lett. 5 (2018) 487–494, https://doi.org/10.1021/acs.estlett.8b00366.
[2] T. Batakliev, V. Georgiev, M. Anachkov, S. Rakovsky, G.E. Zaikov, Ozone decomposition, Interdiscip. Toxicol. 7 (2014) 47–59, https://doi.org/10.2478/intox-2014-0008.
[3] C. Guo, Z. Gao, J. Shen, Emission rates of indoor ozone emission devices: a literature review, Build. Environ. 158 (2019) 302–318, https://doi.org/10.1016/j.buildenv.2019.05.024.
[4] R. Cao, P. Zhang, Y. Liu, X. Zheng, Ammonium-treated birnessite-type MnO_2 to increase oxygen vacancies and surface acidity for stably decomposing ozone in humid condition, Appl. Surf. Sci. 495 (2019), 143607, https://doi.org/10.1016/j.apsusc.2019.143607.
[5] H. Peeters, M. Keulemans, G. Nuyts, F. Vanmeert, C. Li, M. Minjauw, C. Detavernier, S. Bals, S. Lenaerts, Sa.W. Verbruggen, Plasmonic gold-embedded TiO_2 thin films as photocatalytic self-cleaning coatings, Appl. Catal. B Environ. 267 (2020), 118654, https://doi.org/10.1016/j.apcatb.2020.118654.
[6] H. Li, Z. Bian, J. Zhu, Y. Huo, H. Li, Y. Lu, Mesoporous Au/TiO_2 nanocomposites with enhanced photocatalytic activity, J. Am. Chem. Soc. 129 (2007) 4538–4539, https://doi.org/10.1021/ja069113u.
[7] P. Fu, P. Zhang, J. Li, Photocatalytic degradation of low concentration formaldehyde and simultaneous elimination of ozone by-product using palladium modified TiO_2 films under UV254+185nm irradiation, Appl. Catal. B Environ. 105 (2011) 220–228, https://doi.org/10.1016/j.apcatb.2011.04.021.
[8] Y. Zhang, M. Wu, Y.H. Kwok, Y. Wang, W. Zhao, X. Zhao, H. Huang, In-situ synthesis of heterojunction TiO_2/MnO_2 nanostructure with excellent performance in vacuum ultraviolet photocatalytic oxidation of toluene, Appl. Catal. B Environ. 258 (2019), 118034, https://doi.org/10.1016/j.apcatb.2019.118034.
[9] H.U. Lee, S.C. Lee, S.H. Choi, B. Son, S.J. Lee, H.J. Kim, J. Lee, Highly visible-light active nanoporous TiO_2 photocatalysts for efficient solar photocatalytic applications, Appl. Catal. B Environ. 129 (2013) 106–113, https://doi.org/10.1016/j.apcatb.2012.09.010.
[10] A.R. González-Elipe, J. Soria, G. Munuera, Photo-decomposition of ozone on TiO_2, Z. Phys. Chem. 126 (1981) 251–257, https://doi.org/10.1524/zpch.1981.126.2.251.
[11] M.D. Hernández-Alonso, J.M. Coronado, A. Javier Maira, J. Soria, V. Loddo, V. Augugliaro, Ozone enhanced activity of aqueous titanium dioxide suspensions for photocatalytic oxidation of free cyanide ions, Appl. Catal. B Environ. 39 (2002) 257–267, https://doi.org/10.1016/S0926-3373(02)00119-4.
[12] M. Nicolas, M. Ndour, O. Ka, B.D. Anna, C. George, Photochemistry of atmospheric dust: ozone decomposition on illuminated titanium dioxide, Environ. Sci. Technol. 43 (2009) 7437–7442, https://doi.org/10.1021/es901569d.
[13] B. Ohtani, S.W. Zhang, S. Nishimoto, T. Kagyia, Catalytic and photocatalytic decomposition of ozone at room temperature over titanium(IV) oxide, J. Chem. Soc., Faraday Trans. 88 (1992) 1049–1053, https://doi.org/10.1039/FT9928801049.
[14] P. He, M. Zhang, D. Yang, J. Yang, Preparation of Au-loaded TiO_2 by photochemical deposition and ozone photocatalytic decomposition, Surf. Rev. Lett. 13 (2006) 51–55, https://doi.org/10.1142/S0218625×06007810.
[15] K. Cho, K. Hwang, T. Sano, K. Takeuchi, S. Matsuzawa, Photocatalytic performance of Pt-loaded TiO_2 in the decomposition of gaseous ozone, J. Photochem. Photobiol. A Chem. 161 (2004) 155–161, https://doi.org/10.1016/S1010-6030(03)00287-9.
[16] J. Kim, P. Zhang, J. Li, J. Wang, P. Fu, Photocatalytic degradation of gaseous toluene and ozone under $UV_{254+\ 185\ nm}$ irradiation using a Pd-deposited TiO_2 film, Chem. Eng. J. 252 (2014) 337–345, https://doi.org/10.1016/j.cej.2014.05.015.
[17] J. Patzsch, J.Z. Bloh, Improved photocatalytic ozone abatement over transition metal-grafted titanium dioxide, Catal. Today 300 (2018) 2–11, https://doi.org/10.1016/j.cattod.2017.07.010.

[18] S. Gong, W. Li, Z. Xie, X. Ma, H. Liu, N. Han, Y. Chen, Low temperature decomposition of ozone by facilely synthesized cuprous oxide catalyst, New J. Chem. 41 (2017) 4828–4834, https://doi.org/10.1039/C7NJ00253J.
[19] Y. Lin, C. Lin, Catalytic and photocatalytic degradation of ozone via utilization of controllable nano-Ag modified on TiO_2, Environ. Prog. 27 (2008) 469–502, https://doi.org/10.1002/ep.
[20] J. Hoigné, H. Bader, W.R. Haag, J. Staehelin, Rate constants of reactions of ozone with organic and inorganic compounds in water-III. Inorganic compounds and radicals, Water Res. 19 (1985) 993–1004, https://doi.org/10.1016/0043-1354(85)90368-9.
[21] D. Hwang, A.M. Mebel, Ab initio study on the reaction mechanism of ozone with the chlorine atom, J. Chem. Phys. 109 (1998) 10847–10852, https://doi.org/10.1063/1.477781.
[22] R. Yuan, T. Chen, E. Fei, J. Lin, Z. Ding, J. Long, Z. Zhang, X. Fu, P. Liu, L. Wu, Surface chlorination of TiO_2-based photocatalysts: a way to remarkably improve photocatalytic activity in both UV and visible region, ACS Catal. 1 (2011) 200–206, https://doi.org/10.1021/cs100122v.
[23] R. Yuan, S. Fan, H. Zhou, Z. Ding, S. Lin, Z. Li, Z. Zhang, C. Xu, L. Wu, X. Wang, Chlorine-radical-mediated photocatalytic activation of C-H bonds with visible light, Angew. Chem. 125 (2013) 1069–1073, https://doi.org/10.1002/ange.201207904.
[24] X. Fu, W.A. Zeltner, Q. Yang, M.A. Anderson, Catalytic hydrolysis of dichlorodifluoromethane (CFC-12) on sol-gel-derived titania unmodified and modified with H_2SO_4, J. Catal. 168 (1997) 482–490, https://doi.org/10.1006/jcat.1997.1660.
[25] M. Radoičić, G. Ćirić-Marjanović, V. Spasojević, P. Ahrenkiel, M. Mitrić, T. Novaković, Z. Šaponjić, Superior photocatalytic properties of carbonized PANI/TiO_2 nanocomposites, Appl. Catal. B Environ. 213 (2017) 155–166, https://doi.org/10.1016/j.apcatb.2017.05.023.
[26] G. Tian, H. Fu, L. Jing, C. Tian, Synthesis and photocatalytic activity of stable nanocrystalline TiO_2 with high crystallinity and large surface area, J. Hazard. Mater. 161 (2009) 1122–1130, https://doi.org/10.1016/j.jhazmat.2008.04.065.
[27] G. Zhu, J. Zhu, W. Jiang, Z. Zhang, J. Wang, Y. Zhu, Q. Zhang, Surface oxygen vacancy induced α-MnO_2 nanofiber for highly efficient ozone elimination, Appl. Catal. B Environ. 209 (2017) 729–737, https://doi.org/10.1016/j.apcatb.2017.02.068.
[28] C. Zhou, D. Huang, P. Xu, G. Zeng, J. Huang, T. Shi, C. Lai, C. Zhang, M. Cheng, Y. Lu, Efficient visible light driven degradation of sulfamethazine and tetracycline by salicylic acid modified polymeric carbon nitride via charge transfer, Chem. Eng. J. 370 (2019) 1077–1086, https://doi.org/10.1016/j.cej.2019.03.279.
[29] N. Chang, Y. Chen, F. Xie, Y. Liu, H. Wang, Facile construction of Z-scheme AgCl/Ag-doped-ZIF-8 heterojunction with narrow band gaps for efficient visible-light photocatalysis, Coll. Surf. A Physicochem. Eng. Asp. 616 (2021), 126351, https://doi.org/10.1016/j.colsurfa.2021.126351.
[30] R. Song, H. Wang, M. Zhang, Y. Liu, X. Meng, S. Zhai, C.C. Wang, T. Gong, Y. Wu, X. Jiang, Near-infrared light-triggered chlorine radical (.Cl) stress for cancer therapy, Angew. Chem. 132 (2020) 21218–21226, https://doi.org/10.1002/ange.202007434.
[31] Y. Ji, J. Bai, J. Li, T. Luo, L. Qiao, Q. Zeng, B. Zhou, Highly selective transformation of ammonia nitrogen to N_2 based on a novel solar-driven photoelectrocatalytic-chlorine radical reactions system, Water Res. 125 (2017) 512–519, https://doi.org/10.1016/j.watres.2017.08.053.
[32] X. Wang, C.Y. Jimmy, P. Liu, X. Wang, W. Su, X. Fu, Probing of photocatalytic surface sites on SO_4^{2-}/TiO_2 solid acids by in situ FT-IR spectroscopy and pyridine adsorption, J. Photochem. Photobiol. A Chem. 179 (2006) 339–347, https://doi.org/10.1016/j.jphotochem.2005.09.007.
[33] M. Takeuchi, G. Martra, S. Coluccia, M. Anpo, Investigations of the structure of H_2O clusters adsorbed on TiO_2 surfaces by near-infrared absorption spectroscopy, J. Phys. Chem. B 109 (2005) 7387–7391, https://doi.org/10.1021/jp040630d.
[34] E. Rytter, S. Kvisle, Spectral evidence for dimerization of titanium tetrachloride at cryogenic temperatures, Inorg. Chem. 24 (1985) 639–640, https://doi.org/10.1021/ic00199a001.
[35] H. Li, T. Hu, N. Du, R. Zhang, J. Liu, W. Hou, Wavelength-dependent differences in photocatalytic performance between BiOBr nanosheets with dominant exposed (0 0 1) and (0 1 0) facets, Appl. Catal. B Environ. 187 (2016) 342–349, https://doi.org/10.1016/j.apcatb.2016.01.053.
[36] R. Yang, X. Lu, X. Huang, Z. Chen, X. Zhang, M. Xu, Q. Song, L. Zhu, Bi-component Cu_2O-CuCl composites with tunable oxygen vacancies and enhanced photocatalytic properties, Appl. Catal. B Environ. 170–171 (2015) 225–232, https://doi.org/10.1016/j.apcatb.2015.01.046.
[37] J. Guo, L. Mao, J. Zhang, C. Feng, Role of Cl^- ions in photooxidation of propylene on TiO_2 surface, Appl. Surf. Sci. 256 (2010) 2132–2137, https://doi.org/10.1016/j.apsusc.2009.09.062.
[38] Z. Cao, T. Zhang, P. Ren, D. Cao, Y. Lin, L. Wang, B. Zhang, X. Xiang, Doping of chlorine from a neoprene adhesive enhances degradation efficiency of dyes by structured TiO_2-coated photocatalytic fabrics, Catalysis 10 (2020) 69, https://doi.org/10.3390/catal10010069.
[39] M.B. McElroy, R.J. Salawitch, S.C. Wofsy, J.A. Logan, Reductions of antarctic ozone due to synergistic interactions of chlorine and bromine, Nature 321 (1986) 759–762.
[40] Y. Liu, G. Xu, Q. Sha, ESR study on the photolysis of chlorohydrocarbons, Acta Phys. Chim. Sin. (1989) 525–530.
[41] Y. Li, W. Nie, Y. Liu, D. Huang, Z. Xu, X. Peng, C. George, C. Yan, Y.J. Tham, C. Yu, Photoinduced production of chlorine molecules from titanium dioxide surfaces containing chloride, Environ. Sci. Technol. Lett. 7 (2020) 70–75, https://doi.org/10.1021/acs.estlett.9b00704.
[42] M.J. Molina, F.S. Rowland, Stratospheric sink for chlorofluoromethanes: chlorine atomc-atalysed destruction of ozone, Nature 249 (1974) 810–812.